Materials Research. 2012; 15(5): 763-769
DOI: 10.1590/S1516-14392012005000103

Study of the Al-Si-X System by Different Cooling Rates and Heat Treatment

***Miguel Angel Suarez*[a]*, *Ignacio Figueroa*[b], *Alejandro Cruz*[a], *Alfredo Hernandez*[a], *Jose Federico Chavez*[a]**

[a]*Departamento de Ingeniería en Metalurgia y Materiales, Instituto Politécnico Nacional, Escuela Superior de Ingeniería Química e Industrias Extractivas – ESIQIE, UPALM, 07738, México, D. F., México*
[b]*Instituto de Investigaciones en Materiales, Universidad Nacional Autónoma de México – UNAM, Circuito Exterior, s/n, Cd. Universitaria, C.P. 04510, México, D. F., México*

Received: December 6, 2011; Revised: April 16, 2012

The solidification behavior of the Al-12.6% Si (A1), the hypereutectic Al-20%Si (A2) and the Al-20%Si-1.5% Fe-0.5%Mn (A3) (in wt. (%)) alloys, at different cooling rates is reported and discussed. The cooling rates ranged between 0.93 °C/s and 190 °C/s when cast in sand and copper wedge-shaped molds, respectively. A spheroidization heat treatment was carried out to the alloys in the as-cast condition at 540 °C for 11 hours and quench in water with a subsequent heat treatment at 170 °C for 5 hours with the purpose of improving the mechanical properties. The samples were characterized by optical microscopy, scanning electron microscopy and mechanically by tensile test, in order to evaluate the response of the heat treatment on the different starting microstructures and mechanical properties. It was found that alloys cooled at rates greater than 10.8 °C/s had a smaller particle size and better distribution, also showed a greater response to spheroidization heat treatment of all silicon (Si) phases. The spheroidization heat treatment caused an increase in the ultimate tensile stress (UTS) and elongation when compared with the alloys in the as-cast condition. The highest UTS value of 174 MPa was obtained for the (A1) alloy.

Keywords: *aluminum alloys, cooling rates, heat treatment, particle size, mechanical properties*

1. Introduction

Aluminum-Silicon (Al-Si) alloys are the most important of the Al alloys, these are classified in three groups: hypoeutectic (<11 wt. (%) Si), eutectic (11-13 wt. (%) Si), and hypereutectic (>13 wt. (%) Si). The hypereutectic alloys are attractive to the automotive industry and desirable for wear resistant applications, where high strength and low weight ratio are required[1,2]. The microstructures of the hypereutectic Al-Si alloys could be considered as metal-matrix composites (MMC) reinforced by hard particles. Previous studies have reported that the mechanical properties of Al-Si alloys depend on several microstructural parameters such as grain size, secondary dendrite arm spacing (SDAS), distribution of hard phases, the presence of secondary phases or Fe - intermetallic compounds, the morphology of Si particles (size, shape and distribution) and porosity. These are associated with the alloy composition, eutectic modification, degassing and solidification rates[3-7].

In spite of the advantages of hypereutectic Al-Si alloys, their insufficient strength, low ductility and low fracture toughness impede efforts to widen their applications[8]. Therefore, an important scientific task could be the optimization of the casting and solidification processes to enhance the aforementioned properties. Poor ductility was found in microstructures solidified at low cooling rates (>1 °C/s) that showed an overgrowth of primary Si in the Al matrix, as well as a large fraction of coarse acicular eutectic Si. On the other hand, rapid cooling may produce fragility in thin-section castings[9].

In order to minimize the above-mentioned problems and to improve the mechanical properties, several solutions such as addition of alloying elements, control of the solidification rates and performing different heat treatments have been proposed[10].

Spheroidization heat treatment may improve the mechanical properties of the alloy by increasing the elongation, without a loss in mechanical strength. The resultant microstructure is characterized by spheroidized Si particles, which lead to less stress concentration when compared to acicular Si morphologies. During the heat treatment, the morphology of the eutectic Si is modified from needle shaped to a more spherical geometries[11]. In addition, the spheroidized Si particles and refined precipitates can provide a retard in cracks nucleation, resulting in a much-improved casting ductility[12].

Semi-rapid solidification rates may be adequate to induce microstructural changes such as refinement of phases, including the Fe-Si intermetallic compounds, increasing the solubility of some elements in the matrix, modification of acicular eutectic silicon and suppress the formation

*e-mail: msuarez@iim.unam.mx

of detrimental precipitates[13-15]. Besides, the modified microstructures, by the effect of cooling, have shown a positive response to the subsequent heat treatment, which gives them the final mechanical properties.

The objective of the present work is to evaluate the effect of cooling rates and the spheroidization heat treatment on the microstructures of Al-Si alloys: (A1) Al-12.6 wt. (%) Si, (A2) Al-19 wt. (%) Si and (A3) Al-19%Si-1.5%Fe-0.5%Mn to determine the best microstructural morphology in order to improve the mechanical properties. For this purpose, the alloys were solidified in different molds: sand, iron and a cooper wedge-shaped mo ld. The A3 alloy with the same Si level (20 wt. (%)) that the A2 alloy but with higher iron level, was also proposed in order to study the effect of Fe-intermetallic compounds on the microstructure and mechanical properties.

2. Experimental Procedure

The Al-12.6Si, Al-20Si and Al-20Si-1.5Fe-1.5Mn (in wt. (%)) alloys denoted in this work as A1, A2 and A3 respectively, were produced with commercial pure metals (99.8%) in a gas furnace. Before casting, the melts were degassed with hexachloroethane to reduce the hydrogen levels and then a commercial Al-Ti-B alloy was added for grain refinement.

For achieving different cooling rates, the alloys were poured into rectangular molds of different heat extraction media i.e. sand and iron. Mold dimensions are 10 × 1 × 6 cm (long, wide and height). For semi-rapid and rapid solidification, a 2.5 cm thickness wedge-shaped copper mold with a cavity angle of 7° and 1 × 10 × 10 cm (long, wide and height) was used. The chemical composition of the alloys was analyzed by optical emission spectroscopy (OES), and the results are shown in Table 1.

After casting, the alloys were heat treated for 11 hours at 540 °C in a tube furnace followed by quenching into a water container, and then the alloys were heated at 250 °C for 3 hours to modify the Si phases. The samples were metallographically prepared up to 4000 grade SiC paper, and polished with Al_2O_3 particles of 0.5 μm before the microstructural analysis. The microstructures were analyzed by optical microscopy (OM) and scanning electron microscopy (SEM). In addition, punctual SEM-microanalysis was carried out for analyzing and identification of phases.

Additional ingots were solidified at the same cooling rate reached in the upper part of the wedge-shape mold by using a rectangular copper mold to provide samples for the mechanical properties evaluation. Rectangular tensile specimens (with total length = 10 cm, width = 0.64 cm, thickness = 0.6 cm and gauge length = 2.54 cm) were machined according to the ASTM-E8 standard. All tensile tests were performed at room temperature using a 10 t Shimatzu AG-100 electromechanical machine with a fixed cross head speed of 0.5 s-1.

Table 1. Investigated alloy compositions in wt. (%).

Alloys	Si	Fe	Mn	Al
A1	12.9 ± 0.2	0.213 ± 0.1	0.0035 ± 0.002	Balance
A2	19.8 ± 0.2	0.223 ± 0.1	0.0056 ± 0.002	Balance
A3	19.6 ± 0.2	1.3 ± 0.1	0.58 ± 0.002	Balance

3. Results and Discussion

3.1. *Microstructural characterization of alloys in the as-cast condition*

Figure 1 shows the optical micrographs of the alloys that were solidified at slow cooling rates. Figure 1a-c represents the microstructures solidified in sand mold, while Figures 1d-f represents the microstructures solidified in an iron mold. Figure 1a shows the microstructural features of A1 alloy. The microstructure consisted mainly of large acicular eutectic (Al + Si) and small particles of pro-eutectic Si, with an average size of 442 ± 3.2 μm^2 distributed in the Al matrix. The A2 alloy microstructure was mainly constituted by coarse pro-eutectic Si particles with an average size of 2.7 ± 2.2 × 10^4 μm^2 and coarse eutectic (Al + Si) distributed in the Al matrix, as shown in Figure 1b.

The microstructure of the A3 alloy consisted of coarse pro-eutectic Si particles, Fe-intermetallic compounds of light gray color and fine scale ternary eutectic (Al + Si + β) phase, as shown in Figure 1c. The sequence of the solidification indicates that the large Fe-intermetallic compounds (with and average size of 6.7 ± 3.2 × 10^3 μm^2) and coarse pro-eutectic Si phase were formed at the beginning, during slow cooling.

The Al-matrix and the eutectics seem to be formed during the final cooling stage. This figure also shows that the microstructure of the A3 alloy consists of two intermetallic compounds. These compounds are: a) large cube-shaped Fe-intermetallic with a composition of $Al_{46.5}Si_{25}Fe_{26}Mn_{2.5}$ and b) needle-shaped Fe-intermetallic with a composition of $Al_{62.8}Si_{12}Fe_{23}Mn_2$. These compounds were identified by punctual SEM-EDX microanalysis, corresponding to the metastable tetragonal δ-Al_4FeSi_2 and stable monoclinic β-Al_5FeSi intermetallic compounds, respectively.

As it is well known, the manganese (Mn) is able to change the morphology of the iron-rich phase from platelets to a more cubic form or globules[16]. These morphologies drastically improve the tensile strength, elongation, and ductility. However, the coarse Fe intermetallic compounds formed at slow cooling rate are detrimental for the mechanical properties.

The commercially pure Al, usually contains traces of Fe and Mn. The solid solubility of Fe in Al is very low, therefore, high Fe contents tends to form intermetallic compounds[17,18]. The ingot of Al used to produce the master alloy contained low percentage of Fe ~ 0.2 wt. (%). Although the Fe content was not significant to form the largest intermetallic compounds in A1 and A2 alloys, fine needles-shaped of β-Al_5FeSi phase were formed.

Most coarse pro-eutectic Si particles were observed at the boundaries of intermetallic compounds, indicating that the Fe-intermetallic compound surface may act as a nucleation site.

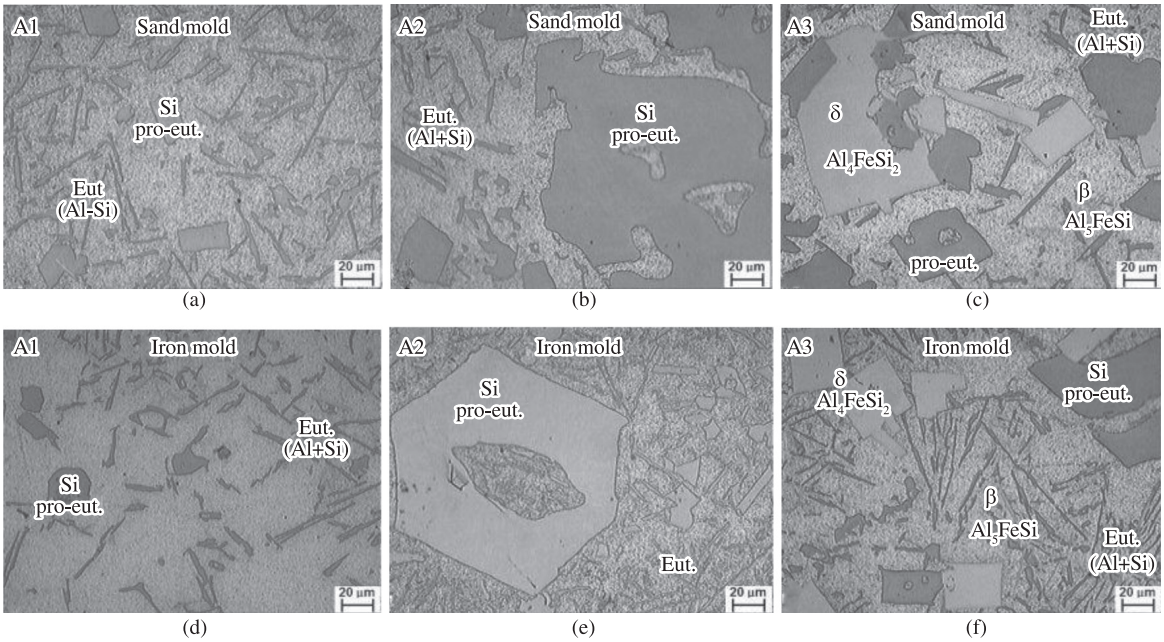

Figure 1. Optical micrographs of the alloys in the as-cast condition: (a-c) alloys solidified in a sand mold and (d-f) alloys solidified in an iron mold.

The microstructures of the alloys solidified in the iron mold (Figures 1d-f) are similar to the alloys solidified in sand molds. When increasing the cooling rate, all the phases that constitute the microstructure decreased in size. The average sizes of pro-eutectic Si in A2 and A3 alloys were $1.8 \pm 1.1 \times 10^4$ and $5.8 \pm 1.1 \times 10^3$ µm^2, respectively. The average size of the cube-shaped intermetallic compound (δ-Al_4FeSi_2) in A3 alloy decreased down to $1.4 \pm 0.5 \times 10^3$ µm^2.

The wedge-shaped ingots provided different cooling rates, allowing the evaluation of the microstructure evolution as a function of chemical composition and cooling rates[19,20]. Figure 2 shows the microstructures of the three alloys obtained in the upper, middle and tip parts of the wedge shaped ingot.

Small pro-eutectic Si particles and eutectic Al + Si, distributed in the Al-matrix, constituted the microstructure of the A1 alloy solidified in the upper part of the ingot. The A2 alloy showed pro-eutectic Si particles (average size 338 ± 2.3 µm^2) and the eutectic (Al + Si) phase in the Al-matrix, while the A3 alloy was constituted for the same phases that the A2 alloy, plus the Fe-intermetallic compounds. The rod-shaped compounds with an average size of 178 ± 2.3 µm^2 and the needle-shaped compounds were identified as δ-Al_4FeSi_2 and the β-Al_5FeSi, respectively. The higher cooling rates achieved with the wedge shaped mold caused a change in the morphology of the δ-Al_4FeSi_2 phase and a decrease in the magnitude of the β-Al_5FeSi phase when compared with the alloys solidified in sand and iron molds. Besides the above-mentioned predominant Fe-intermetallic compounds, there were found other varieties of Fe-compounds, such as $Al_{60.4}Si_{13.1}Fe_{16.1}Mn_{7.1}Cr_{2.9}$ and fine $Al_{39.8}Si_{29.7}Fe_{27.6}Mn_{2.9}$.

The increase of cooling rate from the upper part toward the tip region caused an increase in the solubility of Si in the Al-matrix and a gradual disappearance of pro-eutectic Si in A1 and A2 alloys. With the increase of cooling rates, the δ-Al_4FeSi_2 and β-Al_5FeSi phases did not disappear but their size decreased. These results were found to be in good agreement with the studies reported by Rajabi et al.[21] and Srivastava et al.[22]. They established that the size and volume fraction of Fe-intermetallic compounds increased when increasing iron content, and decreased when increasing the cooling rate. The persistent pro-eutectic Si particles at the tip of the A3 alloy can be attributed to the presence of fine Fe-intermetallic compounds, which acted as nucleation sites even at high solidification rates.

Regarding the eutectic phase, the cooling rate caused a modification in its morphology. For instance, the microstructure of the alloys cooled in a sand mold, showed a class 1 eutectic (unchanged), while the eutectic formed in the alloys cooled in the central part of copper wedge-shaped mold seemed to be of class 3 (partially modified).

From the optical micrographs the secondary dendrite arm spacing (SDAS) was measured in order to establish the cooling rates of the alloys solidified in different molds. For this purpose, the following equation[23] was employed to calculate the cooling rates, *R*:

$$\log R = -2.5 \log \lambda s + 4.5 \quad (1)$$

where λs is the secondary dendrite arm spacing (in µm), *R* is the cooling rate (in °C/s).

Table 2 shows the cooling rates, calculated using Equation 1, and employing the experimental secondary dendrite arm spacing (SDAS). In the investigated alloy, the increase of the solidification rate resulted in a significant reduction of the SDAS.

The smallest size of SDAS was obtained in the tip region of the cooper wedge-shaped mold for the A3 alloy, whilst

the largest SDAS was observed in the A1 alloy cooled in sand mold. The matrix refinement shown in A3 alloy can be explained by the fact that, the fine Fe-intermetallics compounds were initially formed from the liquid, before the formation of any other phase, and therefore acted as nucleation sites.

3.2. *Characterization microstructural of alloys after heat treatment*

Figure 3 shows the microstructures of the alloys solidified in sand and iron molds after the heat treatment of spheroidization. As can be observed, the eutectic Si with the highest degree of spheroidicity was obtained in the A1 alloy, which was solidified in the iron mold. The eutectic Si of the alloys that were solidified in sand mold was found to be partially espheroidized. This result was attributed to the coarse size of the eutectic Si. The morphology and size of the eutectic Si are important because in a partially modified eutectic, achieved by adding additive elements or by rapid solidification, the initial stages of the heat treatments are short and therefore a more complete transformation will be obtained.

Figure 4 shows the microstructures of the wedge-shaped ingots of the alloys after the spheroidization heat treatment. From these figures, it is possible to observe that the microstructure solidified at high cooling rates, caused a high degree of transformation of the eutectic Si. Besides, high

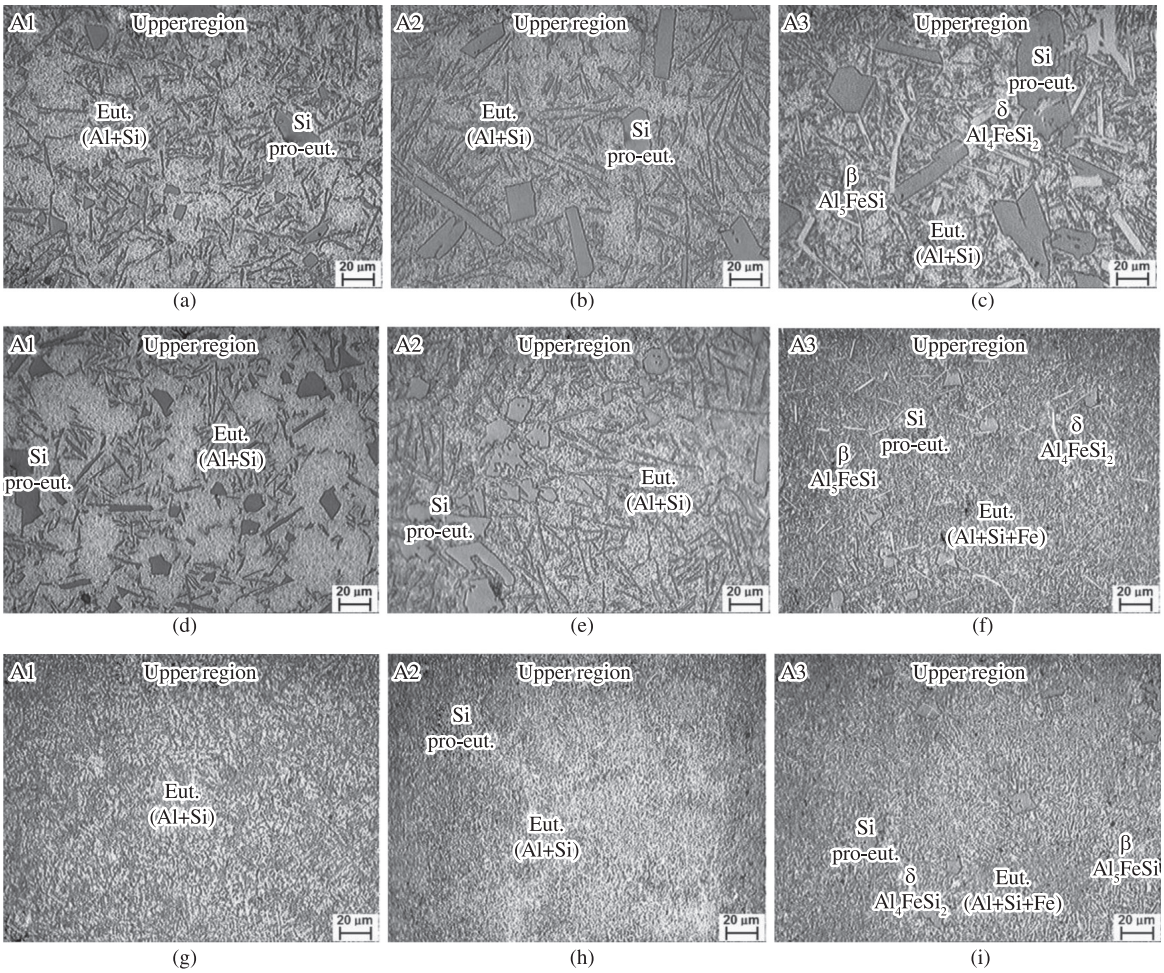

Figure 2. Micrographs of the wedge cast ingots in the as cast condition: (a-c) upper part, (d-f) middle part and (g-i) tip part.

Table 2. Cooling rate (R) as a function of SDAS obtained from Equation 1[16].

Alloy (in wt. (%))	Cooling rate[°C/s]/(SDAS)[µm]				
	Molds		Wedge-shaped mold		
	Sand	Iron	Upper region	Middle region	Tip
A1	0.95/(47.1)	2.9/(30.2)	10.8/(17.8)	22.7/(13.6)	102/(7.4)
A2	1.24/(41.8)	3.6/(27.3)	15.5/(16.5)	34.9/(11.3)	124.2/(6.8)
A3	1.41/(40.5)	4/(26.6)	19.2/(15.2)	51.8/(9.7)	190/(5.6)

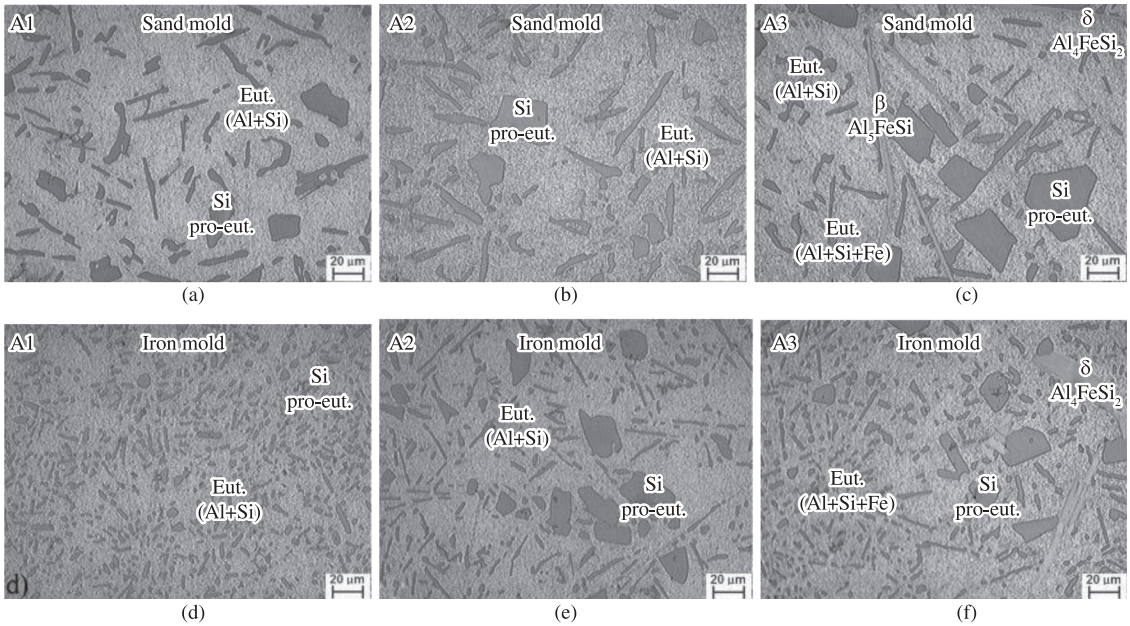

Figure 3. Optical micrographs of the alloys after spheroidization heat treatment: (a-c) solidified in a sand mold; (d-f) solidified in an iron mold.

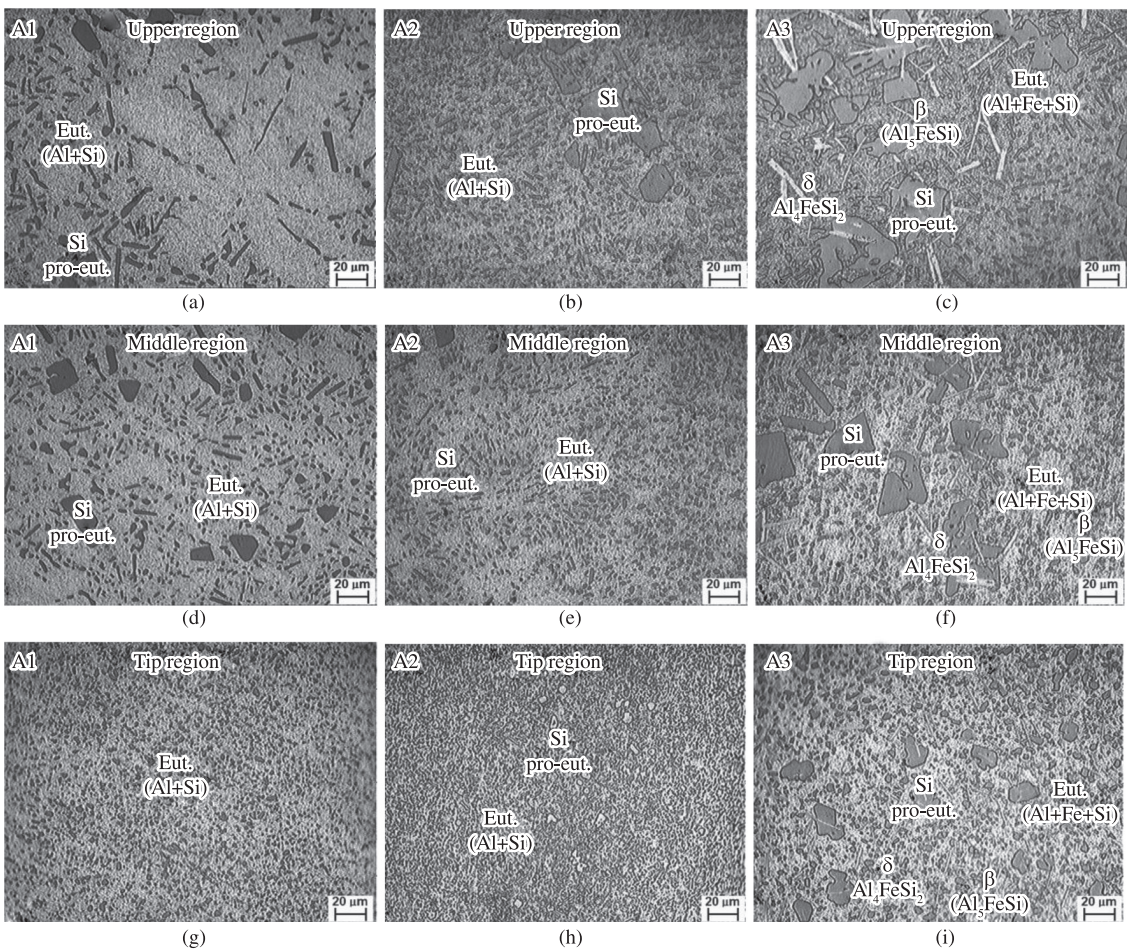

Figure 4. Optical micrographs of the wedge-shaped ingots after spheroidization heat treatment: (a-c) upper part, (d-f) middle part and (g-i) tip part.

cooling rates could refine all phases and drop the amount of Fe-intermetallic compounds. It is also important to point out, that the microstructures of the tip region have a more homogenous distribution of all phases; with the eutectic Si totally spheroidized and with small evidence of the Fe-intermetallic compounds.

3.3. *Evaluation of the mechanical properties*

The tensile test was carried out with samples from the rectangular copper mold that simulates the cooling rate of the upper part of the wedge-shape mold. These samples represent the best condition to be evaluated; since the alloys solidified at slow cooling rates (1.4 < °C/s) are constituted by detrimental coarse phases, and the alloys solidified at high cooling rates (tip, 190 °C/s) showed high contents of Si dissolved in the Al-matrix that provokes fragility in the alloy.

The results of mechanical properties of the as-cast and heat treated alloys are shown in Table 3. For the alloy in the as-cast condition, the A1 alloy showed the highest values of ultimate tensile stress (UTS) and elongation (%) with 141 ± 2.5 MPa and 3.78%, respectively. However, for the A3 alloy with high Si and Fe content, the UTS and the elongation decreased down to 129 ± 2.5 MPa and 1.47%, respectively.

After the spheroidization heat treatment, the mechanical properties of the three alloys increased. The minimum UTS (159 ± 2.5 MPa) and elongation (2.4%) values reached were obtained in A3 alloy, while the maximum values were obtained for the A1 alloy, reaching an elongation up to 6.4% and UTS of 174 ± 2.5 MPa. The highest UTS obtained in the A1 alloy is slightly lower than the results reported by Darvishi et al.[24]. That difference could be attributed to the refinement in their reported microstructure, which was modified with P and Sr additives.

The secondary dendrite arm spacing (SDAS) is not the only factor that affects the mechanical behavior of any given alloy. The A3 alloy with the small SDAS showed the lower UTS and elongation values. This can be attributed to the high iron content that produced a considerably large amount of coarse Fe-intermetallic compounds in the matrix and the small effect of Mn to neutralize the Fe content. When an alloy contains high iron contents, the UTS tends to decrease. Fe-intermetallic compounds are detrimental to the mechanical properties, since its fracture toughness under tensile load is much lower than that for Al matrix or Si particles[25].

Table 3. Results of the mechanical properties of the alloys in the as-cast conditions and after the heat treatment.

Alloy (wt. (%))	SDAS (μm)	As-cast		Heat treatment	
		UTS (MPa)	Elongation (%)	UTS (MPa)	Elongation (%)
A1	19.8	141	3.78	174	6.4
A2	17.7	130	2.45	170	4.07
A3	11	129	1.47	159	2.4

4. Conclusions

The microstructural analysis of Al-12.6% Si (A1), hypereutectic Al-20%Si (A2) and Al-20%Si-1.5% Fe-0.5%Mn (A3) (in wt. (%)) alloys solidified at different cooling rates (1-190 °C/S) was carried out. The cooling rates ranging from 10 °C/s to 50 °C/s favored the formation of microstructures with good distribution of fine pro-eutectic Si and intermetallic compounds. Slow cooling rates (1.4 < °C/s) tended to form detrimental coarse phases, while high cooling rates (190 > °C/s) caused high dissolution of Si contents in the Al-matrix, causing fragility of the alloys and therefore, affecting drastically their mechanical properties.

The spheroidization heat treatment carried out on samples solidified at 10-20 °C/s increased the ultimate tensile stress (UTS) and elongation values compared with the alloys in the as-cast condition. The highest elongation (6.4%) and UTS (174 ± 2.5 MPa) values were obtained for the A1, while the A3 alloy showed the lowest elongation (2.4%) and UTS (159 ± 2.5 MPa) values. This was attributed to the negative effect of the Fe-intermetallic compounds.

Acknowledgements

The authors acknowledge the financial support from Consejo Nacional de Ciencia y Tecnologia (CONACYT) and SIP-IPN. IAF would like to acknowledge the financial support of PAPIIT-UNAM IA101111, IB100712 and SENER - CONACYT 151496 in funding the project. A. Tejeda, C. Flores, G. Aramburo y E. Contreras are also acknowledge for their technical support.

References

1. Hong SJ and Suryanarayana C. Mechanical Properties and Fracture Behavior of an Ultrafine-Grained Al-20 Wt Pct Si Alloy. *Metallurgical and Materials Transactions A*. 2005; 36(3):715-723. http://dx.doi.org/10.1007/s11661-005-0187-z
2. Matsuura K, Kudoh M, Kinoshita H and Takahashi H. Precipitation of Si particles in a super rapidly solidified Al-Si hypereutectic alloy. *Materials Chemistry and Physics*. 2003; 81:393-395. http://dx.doi.org/10.1016/S0254-0584(03)00030-0
3. Ohata Y, Fukui K, Iwai I and Murase I. Development of High Wear Resistance Al-Si Alloy. *Bulletin of the Japan Institute of Metals*. 1985; 24:307. http://dx.doi.org/10.2320/materia1962.24.307
4. Choi YS, Lee JS, Kim WT and Ra HY. Solidification behavior of Al-Si-Fe alloys and phase transformation of metaestable intermetallic compound by heat treatment. *Journal of Materials Science*. 1999; 34:2163-2168. http://dx.doi.org/10.1023/A:1004584415196
5. Zhu MF and Hong CP. Modeling of Irregular Eutectic Microstructures in Solidification of Al-Si Alloys. *Metallurgical*

and Materials Transactions A. 2004; 35(5):1555-1563. http://dx.doi.org/10.1007/s11661-004-0262-x

6. Hogg SC and Atkinson HV. Inhibited Coarsening of a Spray-Formed and Extruded Hypereutectic Aluminum-Silicon Alloy in the Semisolid State. *Metallurgical and Materials Transactions A*. 2005; 36:149-159. http://dx.doi.org/10.1007/s11661-005-0147-7
7. Shabestary SG and Shahri F. Influence of modification, solidification conditions and heat treatment on the microstructure and mechanical properties of A356 aluminum alloy. *Journal of Materials Science*. 2004; 39:2023-2032. http://dx.doi.org/10.1023/B:JMSC.0000017764.20609.0d
8. Basavakumar KG, Mukunda PG and Chakraborty M. Impact toughness in Al-12Si and Al-12Si-3Cu cast alloys-Part 1: effect of process variables and microstructure. *International Journal of Impact Engineering*. 2008; 35:199-205. http://dx.doi.org/10.1016/j.ijimpeng.2007.03.002
9. Abu-Dheir N, Khraisheh M, Saito K and Male A. Silicon morphology modification in the eutectic Al–Si alloy using mechanical mold vibration. *Materials Science and Engineering*: A. 2005; 393:109-117. http://dx.doi.org/10.1016/j.msea.2004.09.038
10. Dwivedi DK, Sharma A and Rajan TV. Influence of Silicon Morphology and Mechanical Properties of Piston Alloys. *Materials and Manufacturing Processes*. 2005; 20:777-791. http://dx.doi.org/10.1081/AMP-200055138
11. Ogris E, Wahlen A, Lüchinger H and Uggowitzer PJ. On the silicon spheroidization in Al–Si alloys. *Journal of Light Metals*. 2002; 2(4):263-269. http://dx.doi.org/10.1016/S1471-5317(03)00010-5
12. Niu XP, Hu BH, Pinwill I and Li H. Vacuum assisted high pressure die casting of aluminum alloys. *Journal of Materials Processing Technology*. 2000; 105:119-127. http://dx.doi.org/10.1016/S0924-0136(00)00545-8
13. Lavernia EJ, Ayers JD and Srivatsan T. Rapid solidification processing with specific application to aluminum alloys. *International Materials Reviews*.1992; 37:1-44. http://dx.doi.org/10.1179/095066092790150885
14. Dasgupta R. Property improvement in Al-Si alloys through rapid solidification processing. *Journal of Materials Processing Technology*. 1997; 72(3):380-384. http://dx.doi.org/10.1016/S0924-0136(97)00198-2
15. Wang F, Yang B, Duan XJ, Xiong BQ and Zhang J.S. The microstructure and mechanical properties of spray deposited hypereutectic Al-Si-Fe alloy. *Journal of Materials Processing Technology*. 2003; 137(1-3):191-194. http://dx.doi.org/10.1016/S0924-0136(02)01074-9
16. Shabestari SG. The effect of iron and manganese on the formation of intermetallic compounds in aluminum-silicon alloys. *Materials Science and Engineering*: A. 2004; 383:289-298.
17. Pat L. Mangonon, P. E. Fasm, The principles of Materials Selection for Engineering Design. *Prentice-Hall International Inc.* 1999: 560-563.
18. Belov NA and Aksenov AA. *Iron in Aluminium Alloys*: Impurity and Alloying Element. New York: Taylor and Francis Inc; 2002.
19. Suarez MA, Alvarez O, Alvarez MA, Rodriguez RA, Valdez S and Juarez JA. Characterization of microstructures obtained in wedge shaped Al-Zn-Mg alloys. *Journal of Alloys and Compounds*. 2010; 492(1-2):373-377. http://dx.doi.org/10.1016/j.jallcom.2009.11.106
20. Triveño Rios C, Bolfarini C, Botta WJ and Kiminami CS. Rapidly Solidified Al-6Si-3Cu alloy. *Materials Science Forum*. 2008; 570:103-108. http://dx.doi.org/10.4028/www.scientific.net/MSF.570.103
21. Rajabi M, Vahidi M, Simchi A and Davami P. Microstructural evolution of Al-20Si-5Fe alloy during rapid solidification and hot consolidation. *Rare Metals*. 2009; 28:639-645. http://dx.doi.org/10.1007/s12598-009-0122-3
22. Srivastava VC, Ghosal P, Ojha SN. Microstructure and phase formation in spray-deposited Al–18%Si–5%Fe–1.5%Cu alloy. *Materials Letters*. 2002; 56:797-801. http://dx.doi.org/10.1016/S0167-577X(02)00616-X
23. Drouzy M and Richard M. Effet des conditions de solidification sur la qualité des alliage de fonderie de A-U5 G T et A-S7 G, estimation des caractéristiques mécaniques. *Fonderie*. 1969; 285:49-56.
24. Darvishi A, Maleki A, Atabaki MM and Zargami M. The mutual effect of iron and manganese on microstructure and mechanical properties of aluminum-silicon alloys. *Association of Metalurgical Engineers of Servia, MJoM.* 2010; 16(1):11-24.
25. Hang JY, Doty HW and Kaufman MJ. The effect of Mn additions on the microstructure and mechanical properties of Al-Si-Cu casting alloys. *Materials Science and Engineering*: A. 2008; 488:496-504. http://dx.doi.org/10.1016/j.msea.2007.12.026